

Fabrication of Fe₃O₄ nanoparticles via an eco-friendly sonochemical route utilizing cleistocalyx operculatus leaf extract: study of properties and application

N. T. Nguyen ^{a,*}, V. A. Nguyen ^b

^a *School of Chemistry and Life Sciences, Hanoi University of Science and Technology, Hanoi, Vietnam;*

^b *Faculty of Technology and Environment, Hanoi Metropolitan University, Hanoi, Vietnam.*

In this study, Fe₃O₄ nanoparticles were synthesized by microwave-assisted green chemistry method using *Cleistocalyx operculatus* leaf extract. The reaction process is simple, environmentally friendly and easy to perform. The characterization of Fe₃O₄ nanoparticles were analyzed by XRD, FT-IR, SEM, TEM analysis methods. The results showed that Fe₃O₄ nanoparticles are spherical, less agglomerated, have a spinel cubic structure and a crystal size of about 12.3 nm. Fe₃O₄ nanoparticles were used as an adsorbent to remove Congo Red dye. The equilibrium adsorption capacity reached 137.9 mg.g⁻¹. From that, it can be concluded that Fe₃O₄ nanoparticles are promising adsorbent for dye removal in water environment.

(Received February 6, 2025; Accepted May 20, 2025)

Keywords: Fe₃O₄ nanoparticles, Ultrasound-assisted green, Dye removal

1. Introduction

Nanomaterials possess many superior properties, making them extremely useful in modern science and technology applications in numerous fields especially environmental field [1-3]. Firstly, with their ultra-small size, nanomaterials have a very large surface area-to-volume ratio. This is highly beneficial in creating efficient water filters, advanced catalysts, and adsorbent materials for environmental treatment. Moreover, the mechanical properties of nanomaterials are superior, with high wear resistance, strength, and hardness. Some nanomaterials are even biocompatible, making them ideal for medical applications such as drug delivery, diagnostics, and disease treatment. Thanks to these exceptional properties, nanomaterials not only improve efficiency in various fields but also create groundbreaking advancements, paving the way for new future possibilities in science and technology [4-5]. The synthesis of nanomaterials has emerged as a cornerstone of nanotechnology, driven by their exceptional optical, electrical, and catalytic properties, which enable transformative applications in energy storage, biomedical engineering, environmental remediation, and sensing technologies [6]. Traditional synthesis methods, such as sol-gel processes, chemical vapor deposition, and hydrothermal techniques, often rely on hazardous chemicals, extreme reaction conditions, and energy-intensive protocols, posing significant environmental and safety risks [5,6]. In contrast, green synthesis—leveraging plant-derived extracts as bio-reductants and stabilizers—has gained prominence as a sustainable, cost-effective, and eco-friendly solution, consistent with the principles of green chemistry and circular economy. Plant-mediated synthesis exploits the rich diversity of phytochemicals, including alkaloids, phenolic acids, saponins, and polysaccharides, which act synergistically to reduce metal precursors, control nucleation, and stabilize nanoparticles [5,7]. For instance, flavonoids in *Justicia spicigera* extract facilitate the reduction of Ag⁺ to Ag⁰ [8]. A critical advantage of plant-based synthesis lies in its ability to fine-tune nanoparticle characteristics—size, crystallinity, and surface charge—through modulation of extract concentration, pH, and reaction temperature [7]. Among many metal oxide nanoparticles synthesized using green methods, Fe₃O₄ nanoparticles stand out for their unique magnetic properties

* Corresponding author: thinh.nguyennhoc@hust.edu.vn
<https://doi.org/10.15251/DJNB.2025.202.559>

and wide range of applications in biomedicine, environmental remediation, and catalysis. Fe₃O₄ nanoparticles, also known as magnetite nanoparticles, exhibit exceptional magnetic properties, chemical stability, and biocompatibility, making them highly attractive for diverse applications. In the biomedical field, Fe₃O₄ nanoparticles are widely used as drug and magnetic hyperthermia agents for hyperthermia-based treatment. The magnetic properties of these nanoparticles enable targeted drug delivery systems, reducing side effects and improving therapeutic efficiency [7,8]. In environmental science, Fe₃O₄ nanoparticles play a vital role in wastewater treatment by adsorbing heavy metals and organic pollutants. Their high surface area and magnetic properties allow them to be easily separated from treated water, offering a reusable and efficient solution for water purification. Additionally, Fe₃O₄ nanoparticles have shown potential as catalysts in chemical reactions, enhancing reaction rates and selectivity due to their unique surface properties [9,10]. *Cleistocalyx operculatus* is a woody plant commonly grown in Southeast Asian countries, especially in Vietnam. *Cleistocalyx operculatus* is widely grown and used for its health benefits, some authors have used *Cleistocalyx operculatus* leaf extracts to synthesize Ag, Fe nanoparticles [11,12]. To the best of our knowledge, there haven't been any reports on synthesis of Fe₃O₄ nanoparticles using *Cleistocalyx operculatus* extraction with ultrasound-assisted. Therefore, this research aims to explore the potential of leaf extracts from *Cleistocalyx operculatus* for the green synthesis of Fe₃O₄ nanoparticles with the assistance of ultrasound. The synthesized Fe₃O₄ nanoparticles were analyzed by XRD, FT-IR, SEM, TEM methods to determine their structural, morphological properties. Furthermore, the potential applications of the synthesized Fe₃O₄ nanoparticles in removal of Congo red were investigated.

2. Experimental

2.1. Materials and method

Preparation of *Cleistocalyx operculatus* leaf extract: The leaves were harvested in Hanoi, Vietnam. First, wash the leaves with tap water and distilled water, then dry them in an oven at 80 °C for 24 hours. Weigh 10 g of dried leaves, put them in a 500 mL cup, add 250 mL of distilled water, then sonicate at 80 °C for 60 minutes in an ultrasonic machine (Elmasonic S100H Ultrasonic Bath). The mixture was then allowed to cool down.

Fe₃O₄ nanoparticles were synthesized according to the process [6] with some changes: certain amount of weigh FeSO₄ and Fe₂(SO₄)₃ with a molar ratio of 1:2, put into a 500 mL glass cup, then add 150 mL of distilled water and 10 mL of *Cleistocalyx operculatus* extract to the mixture and ultrasonicate (Elmasonic S100H Ultrasonic Bath) at 80 °C for 30 minutes. Then slowly drop NH₃ solution into the above mixture until pH = 10, continue to ultrasonicate for 60 minutes at 80 °C. Fe₃O₄ nanoparticles are formed in the form of black precipitate, use a magnet to attract Fe₃O₄ nanoparticles to the bottom of the cup and decant all the water. Then wash the precipitate many times with distilled water to remove unreacted substances until the pH is neutral, then wash again with alcohol. The resulting product is vacuum dried at 90°C for 15 hours.

2.2. Characterization methods

X-ray diffraction patterns of Fe₃O₄ nanoparticles were carried out on a D8 Advance X-ray diffractometer (Bruker) with a CuK α wavelength of 1.5406 Å and a 2 θ scanning angle ranging from 20 ° to 80 °. FT-IR spectra were performed using a Nicolet Nexus 670 instrument. UV-Vis molecular absorption spectra were examined with the UV-VIS spectrophotometer (Agilent 8453). The surface morphology of Fe₃O₄ nanoparticles was investigated using both Hitachi S-4800 FESEM (field emission scanning electron microscope) and JEOL JEM-1010 TEM (transmission electron microscope).

2.3. Adsorption studies

The experiments on the adsorption of Congo red dye onto Fe₃O₄ nanoparticles were conducted as follows: 0.05 g of Fe₃O₄ nanoparticles were added to a triangular flask containing 50 mL of Congo red dye solutions containing different Congo red dye concentrations, and shaken using

a horizontal shaker. After different periods of time, a magnet was used to attract the Fe_3O_4 nanoparticles to the bottom and 5 mL of the supernatant was collected to measure the instantaneous Congo red dye concentration by using the colorimetric method on an UV-Vis spectrophotometer (Agilent 8453) at a wavelength of 464 nm. After determining Congo red concentration, the 5 mL solution was poured back into the triangular flask to continue the adsorption experiment [13]. The instant amount of adsorbed Congo red, denoted by q_t (mg/l), was calculated:

$$q_t = \frac{(C_0 - C_t)V}{W} \quad (1)$$

C_0 : concentration of Congo red dye at the initial time; C_t ($\text{mg}\cdot\text{L}^{-1}$): concentration of Congo red dye at time t , V (L): the volume of Congo red dye solution; and W (g): the mass of Fe_3O_4 nanoparticles.

3. Results and discussion

3.1 X-ray diffraction analysis

The XRD pattern of the obtained Fe_3O_4 nanoparticles is shown in Figure 1. In the pattern, one can see the characteristic peaks of Fe_3O_4 nanoparticles corresponding to the diffraction angles 2θ of 30° ; 35.7° ; 43.8° ; 53.9° ; 57.0° and 62.8° corresponding to the crystal lattice family (220); (311); (400); (422); (511) and (440) of Fe_3O_4 nanoparticles (JCPDS file no: 00-003-0863) [14]. The crystal size of the material is small because the peaks are all broadened. There are any peaks of other phases in the pattern, proving that the synthesized Fe_3O_4 nanoparticles sample has high purity.

Debye–Scherer formula $D=0.9\lambda/\text{cost } \theta$ was employed to calculate the average crystallite size (D) of Fe_3O_4 nanoparticles using the λ of 0.154 nm [15]. The highest intense peak of Fe_3O_4 spectrum, which is (311) was used for the calculation. The calculated results show that the average crystal size of Fe_3O_4 nanoparticles is about 12.3 nm.

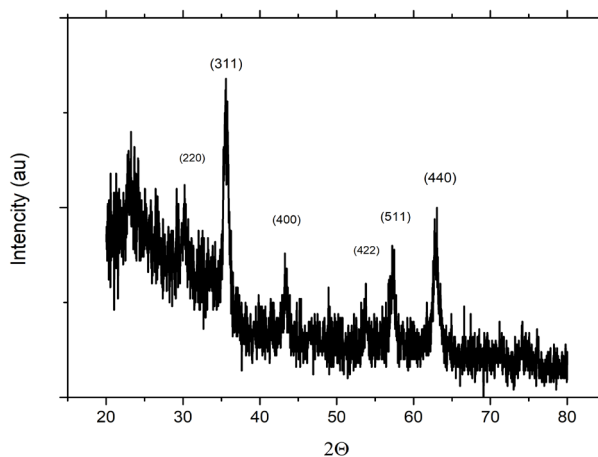


Fig. 1. X-ray diffraction spectra of Fe_3O_4 nanoparticles.

3.2. FT-IR analysis

The FTIR spectrum of Fe_3O_4 nanoparticles is shown in Figure 2, the peak at 3432 cm^{-1} is assigned to the $-\text{OH}$ group of adsorbed water and O-H (polyphenolic group) stretching [16], the peak at 1638 cm^{-1} reveals the existence of the carbonyl group (C=O) [17], and the peak at 580 cm^{-1} on the other hand reveals the existence of the Fe-O group [18,19]. Thus, together with the X-ray diffraction results, it can be confirmed that Fe_3O_4 nanoparticles have been successfully synthesized.

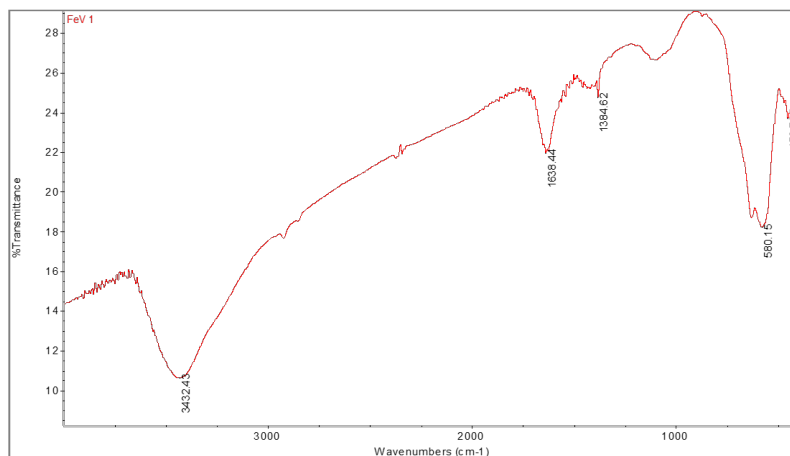


Fig. 2. FT-IR spectra of Fe_3O_4 nanoparticles.

3.3. FESEM analysis

FESEM results of Fe_3O_4 nanoparticles are shown in Figure 3. The spherical Fe_3O_4 nanoparticles is clearly observed. The particles of the green synthesized Fe_3O_4 nanoparticles are uniformly distributed and the smallest size is ~15-20 nm.

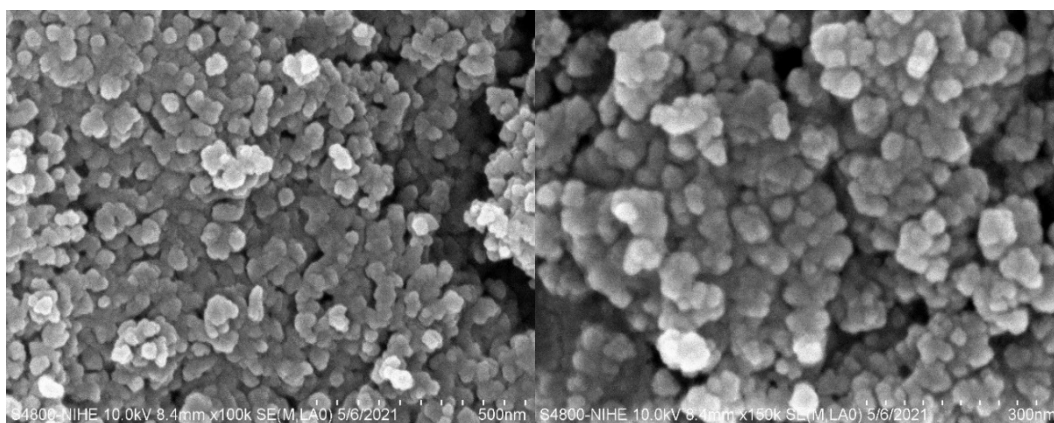


Fig. 3. FESEM images of Fe_3O_4 nanoparticles.

3.4. TEM analysis

TEM scanning electron microscopy results of obtained Fe_3O_4 nanoparticles are shown in Figure 4. The Fe_3O_4 nanoparticles can be seen as spherical shapes with the size of 15-20 nm. It can be seen that green synthesized Fe_3O_4 nanoparticles have less agglomeration phenomenon compared to the previously published synthesis method without using *Cleistocalyx operculatus* leaf extract [6]. Thus, it is possible that the compounds in *Cleistocalyx operculatus* leaf extract have the effect of preventing the agglomeration of Fe_3O_4 nanoparticles.

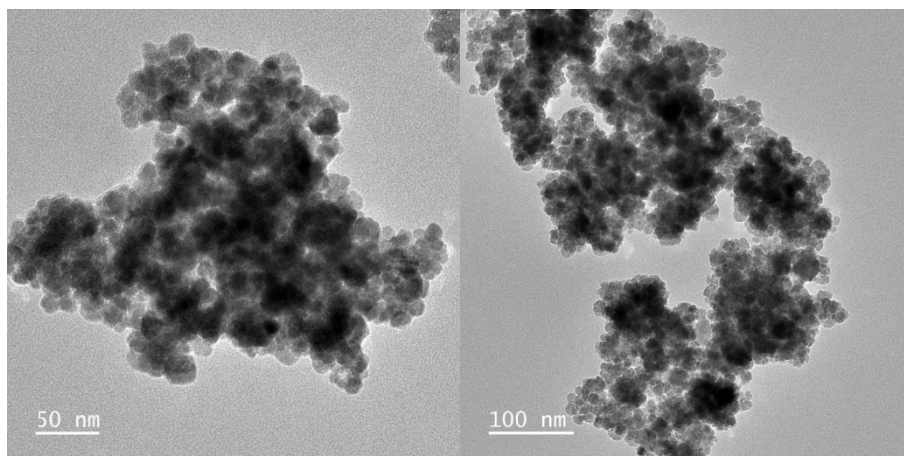


Fig. 4. TEM image of Fe_3O_4 nanoparticles.

3.6. Adsorption studies

The influence of contact time on the ability to remove Congo red of Fe_3O_4 nanoparticles was conducted to discover the equilibrium time to eliminate Congo red. Adsorption experiments were performed within 240 minutes. Figure 5 shows the relationship between adsorption time and removal efficiency of Congo red by Fe_3O_4 nanoparticles. In the first 40 minutes, the removal rate of Congo red increased very quickly, the efficiency reached 81%, then the removal rate gradually decreased and reached 94% after 240 minutes. The rapid adsorption rate at first 40 minutes may due to availability in large quantities of active site on Fe_3O_4 nanoparticles

The mechanism controlling the Congo red adsorption process was examined with different kinetic models including the pseudo-first-order and pseudo-second-order kinetic models.

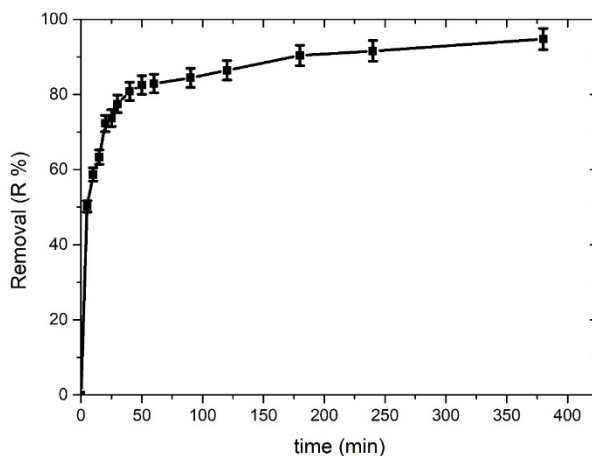


Fig. 5. Adsorption capacity of Congo red dye by Fe_3O_4 nanoparticles as a function of contact time (volume: 50 mL; adsorbent dose: 0.05 g; initial Congo red concentration: 150 mg/L).

Pseudo-first-order and Pseudo-second-order kinetic equations are written as follows [6,13]

$$\log(q_e - q_t) = \log(q_e) - \left(\frac{k_1}{2.303}\right) t \quad (1)$$

$$\frac{t}{q_t} = \frac{1}{k_2 \cdot q_e^2} + \frac{1}{q_e} t \quad (2)$$

in which:

- q_e (mg/g) and q_t (mg/g) are equilibrium and instantaneous adsorption capacity of the material
- k_1 (minute⁻¹): apparent first-order kinetic rate constant
- k_2 (g.mg⁻¹.minute⁻¹): apparent second-order kinetic rate constant.

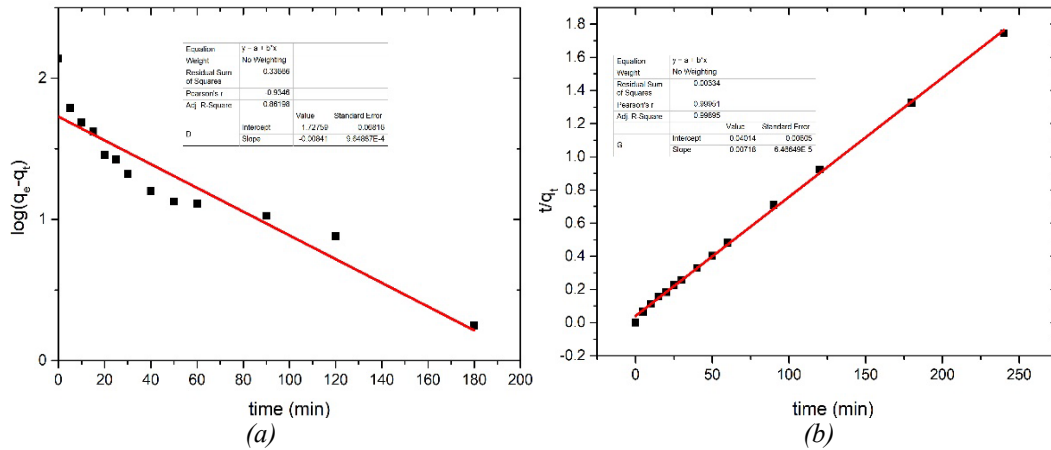


Fig. 6. Pseudo-first-order model (a) and pseudo-second-order model (b) for the adsorption of Congo red by Fe_3O_4 nanoparticles.

Table 1. Pseudo-first-order and pseudo-second-order kinetic model constants.

C_0	$Q_{e,exp}$ (mg/g)	Pseudo-first-order model			Pseudo-second-order model		
		k_1 (min ⁻¹)	$Q_{e,cal}$ (mg/g)	R^2	k_2 (g.mg ⁻¹ min ⁻¹)	$Q_{e,cal}$ (mg/g)	R^2
150 mg/L	137.9	0.0193452	53.407	0.8735	0.001293	138.89	0,999

The equilibrium adsorption capacity $q_{e,cal}$ and the adsorption rate constant k_1 were extrapolated from our data as shown in Figure 6. According to the results, our obtained data do not fit the straight line (Figure 6a). Table 1 compared the theoretical and empirical values of equilibrium adsorption capacity. The first-order kinetic model with parameters $k_1=0.0193452$ min⁻¹ and $q_e=53.407$ mg/g, compared to the experimental q_e cal=137.9 mg/g indicates a substantial deviation between the theoretical and experimental values of the equilibrium adsorption capacity. The theoretical q_e is significantly lower than the experimental value, suggesting that the first-order model underestimates the system's adsorption capacity. Additionally, the coefficient of determination ($R^2=0.8735$) shows a relatively weak correlation between the predicted and experimental data. These data imply that the first-order model is inappropriate to describe the adsorption process's kinetics. This suggests that a different model may provide a more accurate description of the adsorption kinetics. Figure 6b shows the linear relationship between t/q_t and t . The calculated values of k_2 , q_e and their corresponding regression coefficient (R^2) are shown (Table 1). The pseudo-second-order kinetic model, with parameters $k_2=0.001293$ g.mg⁻¹min⁻¹ and $q_{e,cal}=138.89$ mg/g, shows a strong agreement with the experimental $q_e=137.9$ mg/g. The closeness of the theoretical and empirical equilibrium adsorption capacities suggests that the pseudo-second-order model accurately describes the adsorption kinetics for this system. Furthermore, the coefficient of determination ($R^2=0.999$) indicates an almost perfect fit between the predicted and experimental data. This high R^2 value, along with the near-match of q_e values, strongly supports that the adsorption process follows a second-order kinetic mechanism. These results imply that the rate-limiting step of the adsorption process may involve chemisorption, where the adsorption rate is proportional to the square of the number of

active sites available. Overall, the pseudo-second-order model appears to provide a more precise and reliable representation of the system compared to the first-order model.

4. Conclusion

In this study, the green synthesized Fe_3O_4 nanoparticles were successfully synthesized by microwave-assisted precipitation method in *Cleistocalyx operculatus* leaf extract. The green synthesized Fe_3O_4 nanoparticles have a crystal size of 12.3 nm, spherical shape and particle size of about 15-20nm. The obtained Fe_3O_4 nanoparticles were used as adsorbents to treat Congo Red dye. The results showed that the adsorption process of the Congo red on the Fe_3O_4 nanoparticles is better fitted to the second-order kinetic equation than the first-order one. The equilibrium adsorption capacity reached 137.9 mg.g^{-1} .

Acknowledgements

This research is funded by Hanoi University of Science and Technology (HUST) under project number T2024-PC-070

References

- [1] S. Abdolalian, M. Taghavijeloudar, *Journal of Cleaner Production* **365**, 132833 (2022); <https://doi.org/10.1016/j.jclepro.2022.132833>
- [2] F. Shalali, S. Cheraghi, M. A. Taher, *Materials Chemistry and Physics* **278**, 125658 (2022); <https://doi.org/10.1016/j.matchemphys.2021.125658>
- [3] N.T. Nguyen, V.A. Nguyen, *Digest Journal of Nanomaterials and Biostructures* **18** (3), 889 (2023); <https://doi.org/10.15251/DJNB.2023.183.889>
- [4] F. Naserian, A. S. Mesgar, *Colloids and Surfaces B: Biointerfaces* **218**, 112729 (2022); <https://doi.org/10.1016/j.colsurfb.2022.112729>
- [5] A.J. Ruiz-Baltazara, S. Yobanny, R. López, M. L. Mondragón-Sánchez, A.I. Robles-Cortés, R. Pérez, *Results in Physics*, **12**, 989 (2016); <https://doi.org/10.1016/j.rinp.2018.12.037>
- [6] K. C. Paradva, R. Jangir, S. Kalla, *Inorganic Chemistry Communications* **158**(2), 111584 (2023); <https://doi.org/10.1016/j.inoche.2023.111584>
- [7] L. Liu, Y. Li, A.A. AL-Huqail, E. Ali, T. Alkhalifah, F. Alturise, H. E. Ali, *Chemosphere* **334**, 138638 (2023); <https://doi.org/10.1016/j.chemosphere.2023.138638>
- [8] Álvaro de Jesús Ruiz-Baltazar, *Inorganic Chemistry Communications*; <https://doi.org/10.1016/j.inoche.2020.108148>
- [9] Sada Venkateswarlu, B. Natesh Kumar, C. H. Prasad, P. Venkateswarlu, N.V.V. Jyothi, *Physica B* **449**, 67-71, (2014); <http://dx.doi.org/10.1016/j.physb.2014.04.031>
- [10] S. Venkateswarlu, Y. S. Rao, T. Balaji, B. Prathima, N.V.V. Jyothi, *Materials Letters*, **100**, 241, (2013); <https://doi.org/10.1016/j.matlet.2013.03.018>
- [11] T.T.H. Le, T.T. Ngo, T. H. H. Nguyen, T. D. Pham, T.X. H. Vu & Q. V. Tran, *Journal of Inorganic and Organometallic Polymers and Materials* **32**, 547, (2022)
- [12] N. V. Hoang, N.T.X. Quynh, T.D. Dang, T. X Nguyen, V. N Toan, D. D. La, *Chemistryselect* **7** (47), e202203499, (2022); <https://doi.org/10.1002/slct.202203499>
- [13] M. Blachnio, T. M. Budnyak, A. D. Marczevska, A. W. Marczewski, and V. A. Tertykh, *Langmuir* **34** (6), 2258, (2018); <https://pubs.acs.org/doi/10.1021/acs.langmuir.7b04076>
- [14] N. S. Marghaki, Z. AJonoush, A. Rezaee, *Materials Chemistry and Physics* **278**, 125696 (2022); <https://doi.org/10.1016/j.matchemphys.2022.125696>
- [15] Z. Alizadeh, A. Rezaee, *Journal of Molecular Liquids* **366**, 120199, (2022); <https://doi.org/10.1016/j.molliq.2022.120199>

- [16] Bethu, M. S., Netala, V. R., Domdi, L., Tartte, V., Janapala, V. R., *Artificial Cells, Nanomedicine, and Biotechnology* **46** (sup1), 104, (2018); <https://doi.org/10.1080/21691401.2017.1414824>
- [17] Padman, A.J., Henderson, J., Hodgson, S. *et al.* Biomediated synthesis of silver nanoparticles using *Exiguobacterium mexicanum*. *Biotechnol Lett* **36**, 2079–2084 (2014); <https://doi.org/10.1007/s10529-014-1579-1>
- [18] L. Nalbandian, E. Patrikiadou, V. Zaspalis, A. Patrikidou, E. Hatzidaki, C. N. Papandreou, *Current Nanoscience* 12(4),455, (2016); <https://doi.org/10.2174/1573413712666151210230002>
- [19] Lakshmi, K., Rangasamy, R., Prathibha, E. *et al.* *SN Appl. Sci.* **1**, 1121 (2019); <https://doi.org/10.1007/s42452-019-1137-5>